THE JOURNAL OF BIOLOGICAL CHEMISTRY VOL. 283, NO. 29, pp. 19936–19947, July 18, 2008

Prothyrotropin-releasing Hormone Targets Its Processing Products to Different Vesicles of the Secretory Pathway*

Received for publication, January 28, 2008, and in revised form, May 5, 2008 Published, JBC Papers in Press, May 12, 2008, DOI 10.1074/jbc.M800732200

Mario Perello[‡], **Ronald Stuart**[‡], **and Eduardo A. Nillni**[‡§1]

From the [‡]*Division of Endocrinology, Department of Medicine, The Warren Alpert Medical School of Brown University/Rhode Island Hospital, Providence, Rhode Island 02903 and the* [§]*Department of Molecular Biology, Cell Biology, and Biochemistry, Brown University, Providence, Rhode Island 02903*

Prothyrotropin-releasing hormone (pro-TRH) is initially cleaved by the prohormone convertase-1/3 (PC1/3) in the trans-Golgi network generating N- and C-terminal intermediate forms that are then packed into secretory vesicles. However, it is not known whether these peptides are differentially sorted within the secretory pathway. This is of key importance because the processing products of several prohormones fulfill different biological functions. Using AtT20 cells stably transfected with prepro-TRH cDNA, we found that two specific N- and C-terminal peptides were located in different vesicles. Furthermore, the C-terminal pro-TRH-derived peptides were more efficiently released in response to KCl and norepinephrine, a natural secretagogue of TRH. Similar sorting and secretion of N- and C-terminal peptides occurs *in vivo*. When we blocked the initial proteolytic processing by a mutagenic approach, the differential sorting and secretion of these peptides were prevented. In summary, our data show that pro-TRH-derived peptides are differentially sorted within the secretory pathway and that the initial cleavage in the trans-Golgi network is key to this process. This could be a common mechanism used by neuroendocrine cells to regulate independently the secretion of different bioactive peptides derived from the same gene product.

Neuroendocrine cells secrete proteins through two pathways. The first one, the regulated secretory pathway (RSP),[2] stores peptides in secretory granules (SGs) and releases them under external stimulation in a Ca^{2+}-dependent manner (1–3). The second one is the constitutive pathway, which does not store proteins in SGs but instead delivers cargo material in transient vesicles for immediate release. Sorting to the constitutive or regulated pathways begins in the trans-Golgi network (TGN) and/or immature SGs (1, 4–6). The proteolytic processing of many prohormones by prohormone convertases-1/3 (PC1/3) also begins in the TGN (3). Prohormones initially cleaved in the TGN include prothyrotropin-releasing hormone (pro-TRH) (7), prosomatostatin (8), proneurotensin-neuromendin-N (9), procorticotrophin-releasing factor (10), and pro-opiomelanocortin (11–13), although some cases are controversial (14, 15). Thus, we hypothesized that peptides derived from post-translational processing of a given precursor could be differentially sorted within the secretory pathway if the proteolytic processing occurs before to the sorting events.

To test our hypothesis, we used pro-TRH as a model system. We had identified previously the rat pro-TRH (26 kDa) prohormone and its posttranslational processing products (16–18). Pro-TRH is initially cleaved by PC1/3 in the TGN to generate two intermediate forms prior to packing into immature SGs (17, 19, 20). The initial cleavage occurs at two mutually exclusive sites: one generates the 15-kDa and the 10-kDa intermediate peptides, and the alternative cleavage generates 9.5- and 16.5-kDa intermediate peptides (Fig. 1). The 10- and 16.5-kDa C-terminal intermediate forms are further processed to generate shorter C-terminal peptides in the TGN, whereas the 15- and 9.5-kDa N-terminal intermediates appear to undergo processing in a post-TGN compartment, most likely in the immature SGs (21). Initial processing of pro-TRH by PC1/3 in the TGN is also important for downstream sorting events that result in storage of pro-TRH-derived peptides in mature SGs (22). A differential sorting may be critical for pro-TRH, given that, in addition to TRH, other potential bioactive products have been identified (17). For instance, prepro-TRH-(178–199) peptide is increased in the hypothalamus of female rats undergoing suckling; this peptide releases prolactin, which acts directly on pituitary cells (23) and indirectly via inhibition of dopaminergic neurons in the arcuate nucleus (24). Prepro-TRH-(83–106) peptide increases in the periacueductal gray of rats experiencing morphine withdrawal (25). Prepro-TRH-(160–169) peptide regulates TRH-induced thyrotropin secretion from pituitary cells via a specific receptor (26). Thus, the overall goal of this work was to test the hypothesis that N- and C-terminal pro-TRH-derived peptides are differentially sorted within the secretory pathway. Using a combination of *in vitro*, *in vivo*, morphological, biochemical, and mutagenesis approaches, we have demonstrated that the initial processing of pro-TRH in the TGN strongly determine the differential sorting and secretion of pro-TRH peptide products.

* This work was supported, in whole or in part, by National Institutes of Health Grants R01 DK58148 from NIDDK and R01 NS045231 from NINDS (to E. A. N.). This work was also supported by the Dr. George A. Bray Research Scholars Award Fund (to M. P.). The costs of publication of this article were defrayed in part by the payment of page charges. This article must therefore be hereby marked "*advertisement*" in accordance with 18 U.S.C. Section 1734 solely to indicate this fact.

[1] To whom correspondence should be addressed: 55 Claverick St., Rm. 320, Providence, RI 02903. Tel.: 401-444-5733; Fax: 401-444-6964; E-mail: Eduardo_Nillni@brown.edu.

[2] The abbreviations used are: RSP, regulated secretory pathway; SG, secretory granule; PC, prohormone convertase; TGN, trans-Golgi network; RIA, radioimmunoassay; IEM, immunoelectron microscopy; NE, norepinephrine; TRH, thyrotropin-releasing hormone; PBS, phosphate-buffered saline; HPLC, high pressure liquid chromatography; SI, sorting index; aCSF, artificial cerebrospinal fluid; ME, median eminence.

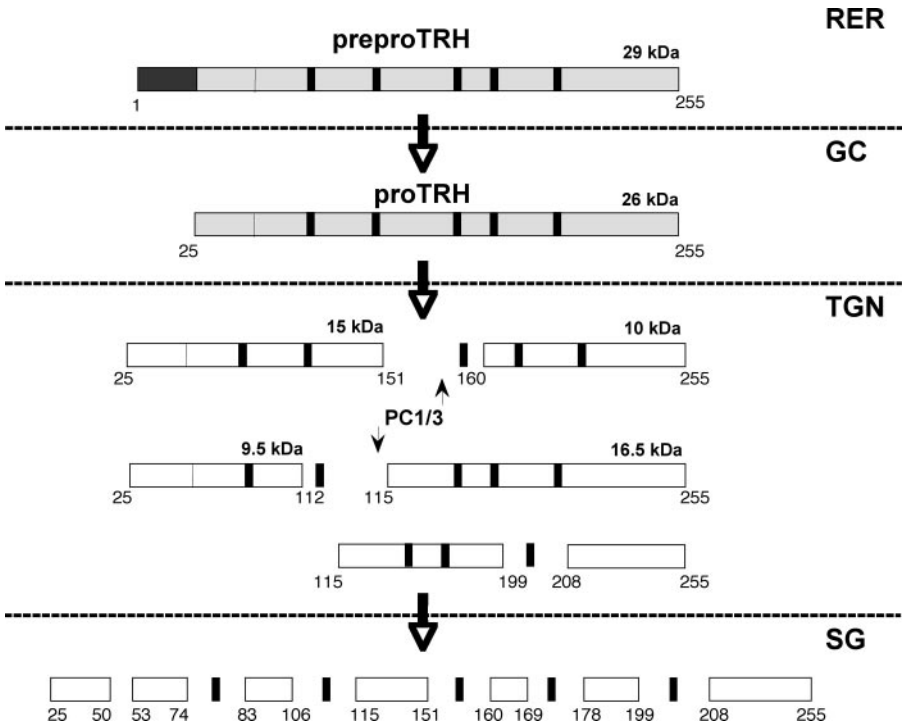

FIGURE 1. **Current model of pro-TRH processing and sorting.** The *light gray rectangles* represent the prepro-TRH and the pro-TRH progenitor sequence (Gln-His-Pro-Gly) is indicated by *black rectangles*; the signal peptide is indicated by the *dark gray rectangle*. *Small numbers below* the peptides indicate the position of the first and last amino acid of the peptide. The signal peptide of the prepro-TRH (29 kDa) precursor is removed in the rough endoplasmic reticulum (*RER*). Then, the pro-TRH (26 kDa) precursor is cleaved at two mutually exclusive sites, primarily by PC1/3. This first step of processing is dependent on PC1/3 and begins in the TGN, generating intermediate forms prior to sorting into immature SGs. After vectorial transport and processing, the final peptide products are found in mature SGs. *Dotted gray lines* separate the different intracellular compartments. *GC*, Golgi Complex.

EXPERIMENTAL PROCEDURES

Antibodies and Materials—The antibody against the N-terminal prepro-TRH_{25-51} sequence (LPEAAQEEGAVTPDLPGLENVQVRPE) plus a tyrosine at the N-terminal end for labeling purposes, named anti-pYE27, and the antibody against the C-terminal prepro-TRH-(239–255) sequence (KQSPQVEPWDKEPLEE) plus a tyrosine added at the N-terminal end, named anti-pYE17, were generated in rabbit and had been characterized previously in our laboratory (20, 21, 23). Anti-pYE27 antibody recognizes only prepro-TRH-(25–50) peptide. Anti-pYE17 antibody can potentially recognize prepro-TRH-(25–255), prepro-TRH-(115–255), prepro-TRH-(160–255), and prepro-TRH-(208–255) peptides (Fig. 1). For electron microscopy studies, antibodies were protein G-purified using protein A/G-agarose from Santa Cruz Biotechnology (Santa Cruz, CA). Unless otherwise specified, all other chemicals and reagents were obtained from Sigma.

In Vitro Studies—AtT20 cells (D16v-F2 subclone; ATCC, Manassas, VA) stably transfected with wild type prepro-TRH or mutant PC1/3-block prepro-TRH cDNAs were generated as described previously (22). In PC1/3-block pro-TRH, basic residues of initial cleavage (prepro-TRH residues 107, 108, 113, 114, 152, 153, 158, and 159) were mutated to glycine residues, which avoid initial processing of the precursor in the TGN. Importantly, this mutated precursor can be processed in other cleavage sites later in the RSP (22). Cells were cultured in Dulbecco's modified Eagle's medium supplemented with high glucose (4.5 g/liter), 30 mM sodium bicarbonate, 1 mM sodium pyruvate, 10% fetal bovine serum, and 0.1% penicillin/streptomycin (Invitrogen) at 37 °C and 5% CO_2. For secretion studies, AtT20 cells were plated in 6-well plates. When cultures were 80% confluent, cells were washed with Hanks' solution and incubated with basal Dulbecco's modified Eagle's medium (2 ml/well, lacking serum and with protease inhibitor mixture (AEBSF: pepstatin A, E64, bestatin, leupeptin, and aprotinin; catalog No. P8340)). After 1 h of incubation, basal medium was collected and replaced with basal, norepinephrine (NE; 50–500 nM)-, or KCl (56 mM)-containing medium (2 ml/well). The NE treatments were based on previous reports (27–29). After 1 h of incubation, stimulated medium was collected, and cells were scraped into cold PBS and pelleted by centrifugation. Cells were lysed by the addition of 500 μl of 2 N acetic acid with protease inhibitor mixture and heated to 95 °C for 10 min. Samples were then sonicated and centrifuged at 15,000 rpm at 4 °C for 30 min. Supernatants were collected, and protein concentrations were determined by Bradford assay (Coomassie protein assay reagent, Pierce). An equal amount of medium (200 μl) or cell extract (4 μg of protein) from each group was evaporated using an Appropriate Technical Resources, Inc. (Laurel, MD) −110 °C speed vacuum system and reconstituted in 1 ml of 0.1% trifluoroacetic acid solution for HPLC separation. Eluted fraction were then evaporated and reconstituted in buffer used for radioimmunoassay (RIA) analysis. Data form basal and KCl-stimulated release were used to calculate the sorting index (SI) as follows: the percentage of total (cell content plus medium) immunoreactive material secreted under nonstimulation condition (basal release) was subtracted from the percentage secreted under KCl stimulation (stimulated release); this value was then divided by the percentage of basal release (30). Samples were run in triplicate per condition in three independent experiments.

For immunoelectron microscopy studies, cells were plated in LabTeks. On the day of the experiment, cells were washed with Hanks' solution and fixed for 1 h with Karnovsky's fixative or 4% paraformaldehyde, 0.15% glutaraldehyde in PBS. Samples were dehydrated with ethanol up to 96% followed by infiltration with LR White acrylic resin, hard grade (London Resin Co.) and embedding under a layer of Aclar film (Electron Microscopy Sciences, Hatfield, PA). Using a Reichert UltraCut S ultramicrotome, thin sections were prepared and placed on 300-mesh uncoated nickel grids for immunogold labeling.

Ex Vivo and in Vivo Studies—Male Sprague-Dawley rats (~250 g) were purchased from Charles River Laboratories, Inc. (Wilmington, MA). The Institutional Animal Care and Use Committee of Rhode Island Hospital/Brown University approved the experimental protocols and euthanasia procedures. Secretion studies were performed in hypothalamic explants. Brains were removed from decapitated rats, placed in a brain matrix (Kent Scientific Corp., Torrington, CT), and cut using optic chiasm as rostral limit and mammillary bodies as caudal limit. Hypothalamic sulci were used as lateral limits, and a 3-mm-thick slice was taken parallel to the base of the hypothalamus. Hypothalamic explants were maintained in a static incubation system using artificial cerebrospinal fluid (aCSF; 126 mM NaCl, 6 mM KCl, 0.09 mM $MgSO_4$, 1.4 mM $CaCl_2$, 0.09 mM Na_2HPO_4, 20 mM $NaHCO_3$, 5 mM glucose, and protease inhibitor mixture, pH 7.4) gassed with 95% O_2 and 5% CO_2. After a 2-h equilibration period, hypothalami were first incubated in 350 μl of basal aCSF for 45 min and then were left untreated with 350 μl of aCSF or treated with NE (50–500 nM)- or KCl (56 mM)-containing aCSF for 45 min. At the end of these experiments, the median eminence (ME) of hypothalamic explants was collected in acetic acid, and peptides were extracted as described above. Samples were loaded into HPLC (300 μl of aCSF, 20 μg of extracted protein) and fractions analyzed by RIA. Samples stimulated with aCSF or KCl aCSF were used to calculate SI as indicated above. This experiment was repeated three times independently, with four samples in each group.

For immunoelectron microscopy studies, animals were processed as described previously (31). Briefly, rats were anesthetized with sodium pentobarbital (50 mg/kg, intraperitoneally), and the heart was exposed and systemically perfused with heparinized saline via the left ventricle followed by Karnovsky's fixative or 4% paraformaldehyde, 0.15% glutaraldehyde in PBS. Brains were carefully removed, and post-fixed for 2 h. Then, 100-μm-thick vibratome coronal sections of hypothalamus were prepared and placed in PBS. Sections were dehydrated and flat embedded as described above. Using a Reichert UltraCut S ultramicrotome, thin sections were prepared and placed on 300-mesh uncoated nickel grids for immunogold labeling.

HPLC Fractionation—A ProStar gradient mode HPLC system equipped with a C18 reverse phase column (Microsorb MV 300-8, 250 × 4.6 mm; Varian Inc., Palo Alto, CA) was used to fractionate samples. For peptide elution, a linear gradient from 0 to 80% of B was used with the following mobile phases: 0.1% trifluoroacetic acid (A) and 90% acetonitrile/0.1% trifluoroacetic acid (B). The flow rate was 1 ml/min, and there were equilibration times used on either side of the gradient. Forty fractions (1 ml) were collected over the entire 40-min gradient. These fractions were then evaporated using a −110 °C speed vacuum system and reconstituted in 210 μl of the buffer used in RIAs. For mass spectrometry, 80 fractions (0.5 ml each) were collected to obtain more pure samples.

Mass Spectrometry—Immunoreactive HPLC fractions of medium samples of AtT20 cells expressing wild type pro-TRH were evaporated and reconstituted in water. One μl of each sample was spotted on a normal phase chip array (NP20, Ciphergen Biosystems, Fremont, CA) as described recently (18). A negative control experiment was done in parallel using the same HPLC separation approach and analyzing medium of untransfected AtT20 cells. Arrays were read using a ProteinChip System, Series 4000 (Ciphergen Biosystems). Spectra of the sample and calibrated standards were generated in auto- mode using the appropriate laser power. Analyses of spectra were accomplished using Ciphergen Express software (version 3.0) (32).

Immunoelectron Microscopy (IEM)—To perform double-sided immunogold labeling, each side of the grid was labeled separately. Sections were blocked with bovine serum albumin and 2% normal goat serum and then incubated with anti-pYE17 antibody (1:50) overnight at 4 °C. Sections were then floated on droplets of 10-nm gold-labeled goat anti-rabbit antibody (Electron Microscopy Sciences/Aurion, Hatfield, PA) for 2 h. Grids were blotted and air-dried. A second label was carried out using anti-pYE27 antibody (1:50) on the opposite side of the grid, avoiding contact with the dry side. After rinsing, sections were incubated with a 25-nm gold-labeled goat anti-rabbit antibody. Following rinses, sections were lightly stained for contrast with aqueous 2% uranyl acetate for 10 min followed by water rinses. Some sections were used to perform controls in which one or both primary antibodies were omitted. Sections were examined using a Morgagni 268 transmission electron microscope, and images were collected with an AMT Advantage CCD camera system. This experiment was repeated on two independent occasions.

Quantitative Analysis of Immunogold Labeling—To perform quantitative analysis, grids were first scanned at low magnification, and then high magnification micrographs were acquired of areas selected on the basis of good overall morphology. Negative and positive vesicles were counted in: (i) 12 section of different cells expressing wild type pro-TRH, (ii) 16 section of different cells expressing PC1/3-block pro-TRH, and (iii) 20 section of the ME. Positive vesicles were considered those that had at least double electron density compared with the background and colloidal gold particles. Gold particles in a ratio of 20 nm outside of a vesicle were considered part of the vesicle based on the minimum theoretical lateral resolution (33). Positive vesicles were counted and organized in three categories: 1) positive for anti-pYE27 antibody; 2) positive for anti-pYE17 antibody; and 3) positive for both antibodies. The relationship was expressed as a percentage, representing the proportion of a particular positive vesicle compared with total number of positive vesicles observed per micrographs. For quantitative analysis, we counted: i) ~980 vesicles of AtT20 cells expressing wild type pro-TRH; ii) ~910 vesicles of AtT20 cells expressing PC1/3-block pro-TRH; and iii) ~600 vesicles of ME. To confirm that the results were not dependent on the size of gold particles, co-staining was also done by using 6- and 10-nm gold-labeled goat anti-rabbit antibodies and by "reverse" staining, shifting the secondary antibodies. All tested variants of the procedure gave similar results. However, the final percentages slightly changed (data not shown) in particular because of the well known higher labeling efficiency of the smaller gold probes (33). The quantitative data shown here was obtained from sections labeled first with anti-pYE17 and 10-nm gold-particles and then with anti-pYE27 and 25-nm gold-particles, because these different size gold particles are more clearly resolved. To

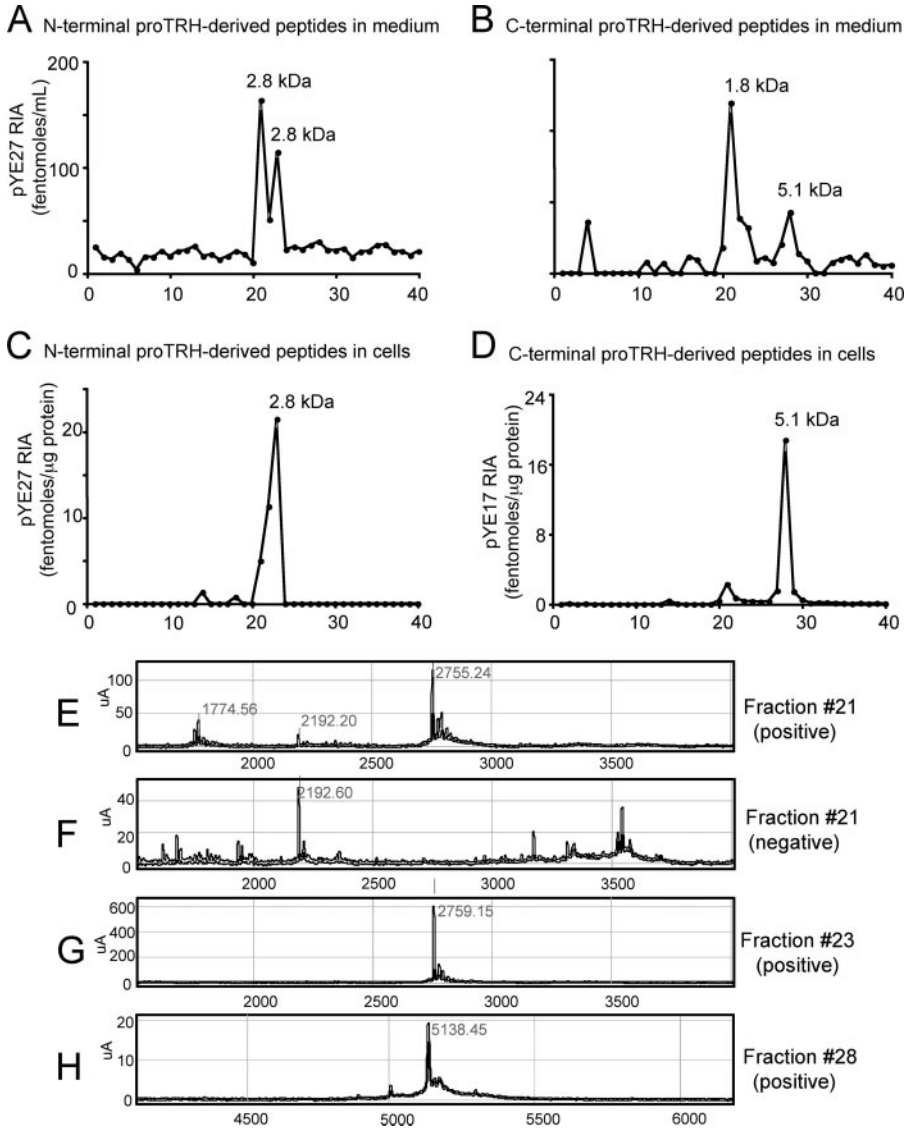

FIGURE 2. **AtT20 cells stably transfected with prepro-TRH cDNA fully process the N- and C-terminal ends of the prohormone.** Medium and cell content were collected and subjected to HPLC purification, and fractions were analyzed using pYE27 and pYE17 RIAs. The *upper panels* show the results of medium samples analyzed with pYE27 (*A*) or pYE17 (*B*) RIAs; the *middle panels* show the results of cell content samples analyzed with pYE27 (*C*) or pYE17 (*D*) RIAs. The *bottom panels* show the profile of the spectra of different immunoreactive medium fractions in the ProteinChip system used to determine the molecular weight. They show fraction 21 of the positive sample (*E*), fraction 21 of the negative sample (*F*), fraction 23 of the positive sample (*G*), and fraction 24 of the positive sample (*H*). On each spectral peak is shown the determined molecular mass.

determine the vesicle diameter we performed point-to-point measurements using Image Capture Engine software, version 5.4.2.271, from Advanced Microscopy Techniques, on the electron microscopic images. Measuring software was calibrated at all magnifications using a diffraction grating replica having 0.463 μ per line (Ernest Fullam Inc., Clifton Park, NY). For quantitative analysis of vesicle diameter we used: i) ~260 vesicles of AtT20 cells expressing wild type pro-TRH (12 sections of different cells); ii) ~270 vesicles of AtT20 cells expressing PC1/3-block pro-TRH (16 sections of different cells); and iii) ~190 vesicles of ME.

Radioimmunoassay—RIAs using anti-pYE27 and anti-pYE17 antibodies were developed in our laboratory and described earlier (19). Customized peptides described above were used as tracers and standards. Tracers were iodinated using the chloramine-T oxidation-reduction method followed by HPLC purification. All RIAs were performed in duplicate. Sensitivity measures of pYE27 and pYE17 RIAs were ~10 and ~5 fmol/tube, respectively. Intra- and interassay variability measures were 5–6 and 9–12%, respectively.

Results are presented as mean ± S.E. Statistical significance was determined by analysis of variance followed by a post hoc Newman-Keuls test. Differences were considered significant at $p < 0.05$.

RESULTS

AtT20 Cells Expressing Pro-TRH Differentially Secrete and Store N- and C-terminal Pro-TRH-derived Peptides—To perform this study, we initially investigated the N- and C-terminal peptides produced in AtT20 cells stably transfected with prepro-TRH cDNA. Medium and cell content were collected and subjected to HPLC purification, and fractions were analyzed using pYE27 and pYE17 RIAs. Analysis of medium samples with pYE27 RIA revealed the presence of two peaks at fractions 21 and 23 (Fig. 2*A*) and one peak at fraction 23 in the cell content samples (Fig. 2*B*). Analysis with pYE17 RIA showed two peaks at fractions 21 and 28 in the medium and cell content samples; the largest peak was at fraction 28 in cell content, whereas in medium the largest peak was at fraction 21 (Fig. 2, *C* and *D*). For pYE17 RIA there was also a small peak in medium samples at fraction 4, most likely unspecific because it was unaffected by treatments (see below). The medium peaks identified with pYE27 and pYE17 RIAs were further analyzed by mass spectrometry. As a negative control we used medium from untransfected AtT20 cells. Analysis of the spectra for fraction 21 showed three peptides with the following molecular masses: 1775, 2192, and 2755 Da (Fig. 2*E*). Fraction 21 of the negative control showed a peptide of 2192 Da, indicating that this is not a pro-TRH-derived peptide (Fig. 2*F*). Thus, the 1775-Da peptide most likely corresponds to prepro-TRH-(241–255) (theoretical molecular mass of 1811 Da) and the 2755-Da peptide to a variant of the N-terminal prepro-TRH-(25–50) (theoretical molecular mass of 2759 Da). Analysis of the spectra for fraction 23 showed one peptide with a molecular mass of 2759 Da,

TABLE 1

Secretion of N- and C-terminal pro-TRH-derived peptides by AtT20 cells stably transfected with wild type prepro-TRH cDNA

The first two columns of values show peptides released after 1 h of treatment with the different secretagogues. They are expressed as the total fmol of N- or C-terminal pro-TRH-derived peptides per ml of medium. Both peptides were measured by RIA. SI was calculated as indicated in the text.

Secretagogue	Pro-TRH-derived peptides in medium		Ratio
	N-terminal	C-terminal	
	fmol/ml		
Basal	255.1 ± 13.9	160.0 ± 7.4[a]	1.59 ± 0.07
NE (50 nM)	423.3 ± 30.8[b]	308.3 ± 40.9[a,b]	1.37 ± 0.18
NE (500 nM)	474.7 ± 56.7[b]	472.3 ± 29.5[b]	1.01 ± 0.13
KCl (56 mM)	587.4 ± 36.9[b]	642.4 ± 57.8[b]	0.91 ± 0.07
SI	1.08 ± 0.13	2.60 ± 0.23[c]	

[a] $p < 0.05$ *vs.* total fmol of N-terminal pro-TRH-derived peptides.
[b] $p < 0.05$ *vs.* basal.
[c] $p < 0.05$ *vs.* SI of N-terminal pro-TRH-derived peptides.

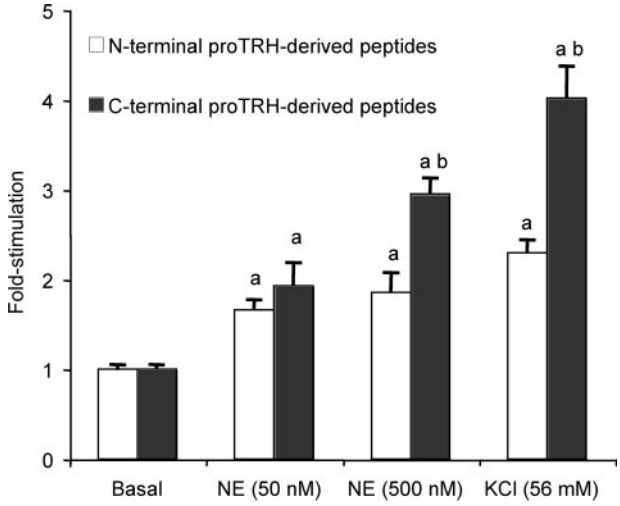

FIGURE 3. **NE and KCl differentially release N- *versus* C-terminal pro-TRH-derived peptides in stably transfected AtT20 cells.** Cells were stimulated with increasing concentrations of NE (50–500 nM) or KCl (56 mM) for up to 1 h. After incubation, medium was processed for HPLC followed by pYE27 and pYE17 RIAs analysis. This figure represents the -fold stimulation for both peptides and for each secretagogue calculated as the total molar amount of peptide in stimulated media/molar amount of peptide in basal media. Data are presented as the mean ± S.E. *a*, $p < 0.05$ *versus* own basal release. *b*, $p < 0.05$ *versus* -fold stimulation of N-terminal pro-TRH-derived peptide for the same stimulus.

which is most likely another variant of the N-terminal prepro-TRH-(25–50) (Fig. 2*G*). Analysis of the spectra for fraction 28 showed one peptide with a molecular mass of 5138 Da, likely corresponding to C-terminal prepro-TRH-(208–255), which has a theoretical molecular mass of 5141 Da (Fig. 2*H*). In the past, we used to call to this peptide the 5.4-kDa C-terminal pro-TRH (17). Fractions 28 and 23 showed no detectable peptides in the negative control (data not shown).

To address whether N- and C-terminal pro-TRH-derived peptides are stored differentially, we investigated their secretion rate in prepro-TRH stably transfected AtT20 cells. The results are expressed as the total number of moles of N- or C-terminal pro-TRH-derived peptides secreted per milliliter (summarized in Table 1) or as -fold simulation (Fig. 3). Under steady state conditions, cell content for the N-terminal peptide was higher than for the C-terminal counterpart (38.0 ± 2.4 *versus* 23.1 ± 0.4 fmol/mg of protein, respectively, $p < 0.05$), and the ratio between N- and C-terminal peptides was 1.64 ± 0.09. Basal secretion for N-terminal peptides was also higher than for C-terminal peptides (255.1 ± 13.9 *versus* 160.0 ± 7.4 fmol/ml, respectively, $p < 0.05$), and the ratio between N- and C- terminal peptides in medium was 1.59 ± 0.07. Fifty and 500 nM NE increased the secretion of N-terminal peptides to 423.3 ± 30.8 and 474.7 ± 56.7 fmol/ml, respectively ($p < 0.05$ *versus* basal) and secretion of the C-terminal peptides to 308.3 ± 40.9 and 472.3 ± 29.5 fmol/ml, respectively ($p < 0.05$ *versus* basal). Calculation of -fold stimulation showed that NE induced more secretion of C- than N-terminal pro-TRH-derived peptides (Fig. 3). To determine the release of these peptides by an unspecific secretagogue, we employed high potassium stimulation. KCl (56 mM) increased the secretion of N- and C-terminal pro-TRH-derived peptides to 587.4 ± 36.9 and 642.4 ± 57.8 fmol/ml, respectively ($p < 0.05$ *versus* basal). As shown in Fig. 3, KCl-induced secretion was more significant for C-terminal than for N-terminal peptides (4.02- ± 0.36-fold *versus* 2.30- ± 0.14-fold, respectively, $p < 0.05$). To assess the regulated release of N- and C-terminal pro-TRH-derived peptides, we calculated the SI, which is a quantitative measure of how well regulated is the secretion of a given peptide (see "Experimental Procedures"). Low SI values indicate that peptides are secreted via the constitutive secretory pathway, and high SI values indicate that secretion is more regulated. SI parameter was higher for C-terminal than for N-terminal peptides (2.60 ± 0.23 *versus* 1.08 ± 0.13, respectively; Table 1, $p < 0.05$) suggesting that C-terminal pro-TRH-derived peptides are more efficiently sorted in SGs than N-terminal peptides.

N- and C-terminal Pro-TRH-derived Peptides Are Located in Different Vesicles of AtT20 Cells Expressing Pro-TRH—We then hypothesized that the non-equimolar release of peptides could be because N- and C-terminal pro-TRH-derived peptides are located in different vesicles. To test this possibility, we used an IEM approach. Under Karnovsky's fixative the ultrastructure of cells was well preserved, but antigenicity was destroyed (data not shown). Therefore, we used a 4% paraformaldehyde/0.15% glutaraldehyde solution that maintained antigenicity and allowed the accurate identification of vesicles (Fig. 4, *A–D*). AtT20 cells expressing wild type pro-TRH showed a total of 42.8 ± 8.2% positive vesicles/cell/section. Positive vesicles were concentrated in three different areas within cells: cytoplasmatic pools in the Golgi region (Fig. 4*A*), small pools close to the plasmatic membrane of the cell body (Fig. 4*B*), and large pools stored in the projections of the cells (Fig. 4*C*). This distribution of vesicles is consistent with previous descriptions (34). Quantitative analysis showed three classes of positive vesicles in steady state conditions (Fig. 4*E*). One class of vesicles was positive for anti-pYE27 antibody and represented 27.2 ± 2.1% of the total positive vesicles. Another class was positive for anti-pYE17 antibody and represented 39.5 ± 4.8% of the total positive vesicles. A third population of vesicles was positive for both antibodies and represented 33.3 ± 3.1% of the total positive vesicles. Mean percentages were obtained for the total number of vesicles because results were not dependent on the location of the pools. The diameter of positive vesicles for anti-pYE27 alone, for anti-pYE17 alone, and for both antibodies were 106.3 ± 3.2, 113.0 ± 2.3, and

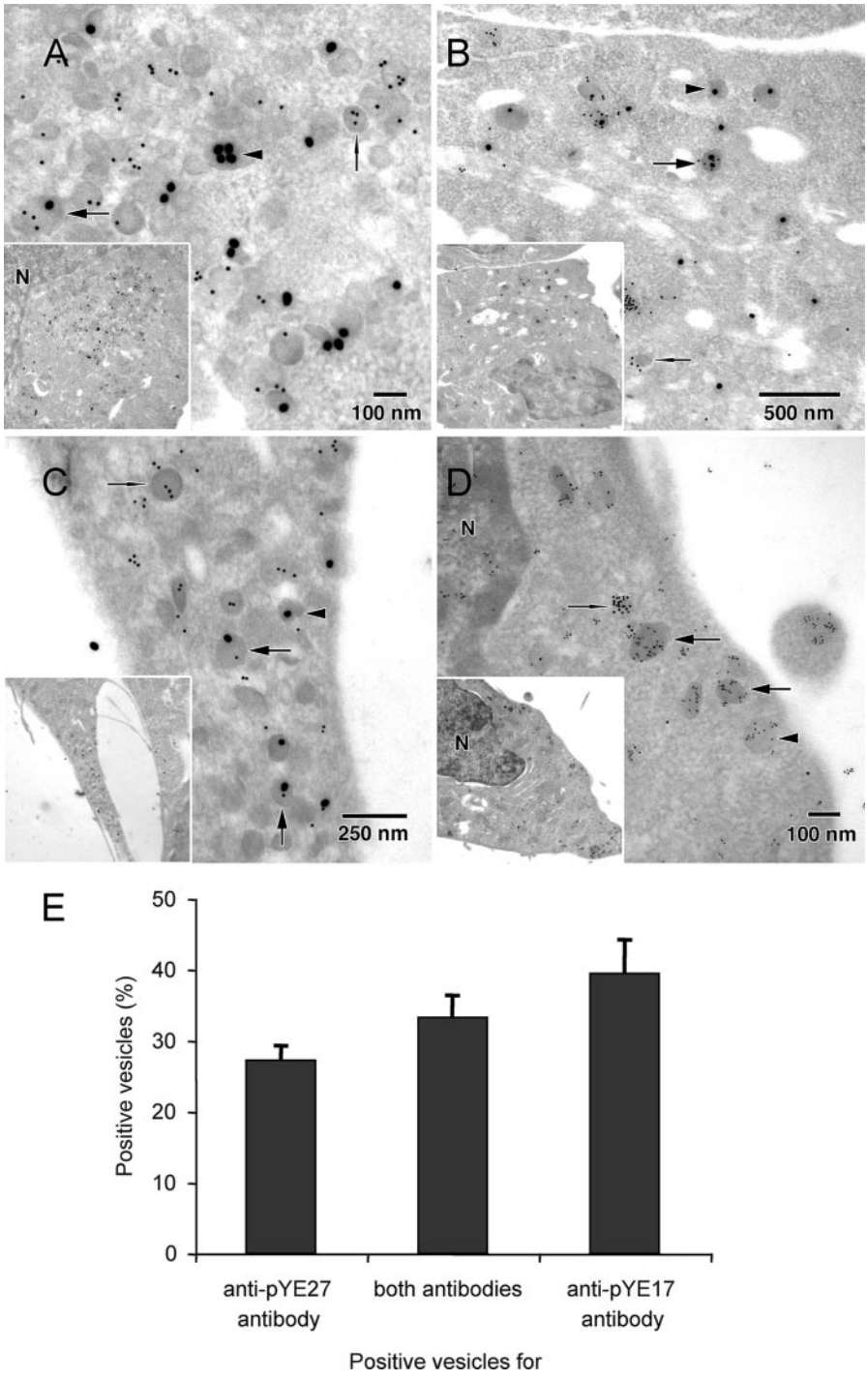

FIGURE 4. **N- and C-terminal end products of pro-TRH processing are targeted to different vesicles in stably transfected AtT20 cells.** Cells were fixed with 4% paraformaldehyde/0.15% glutaraldehyde solution and labeled with anti-pYE17 (visualized with 10-nm gold particle secondary antibody) followed by anti-pYE27 (visualized with 6- or 25-nm gold particle secondary antibody). *A–C* show 10/25-nm gold particle co-staining, and *D* shows 10/6-nm gold particle co-staining. Positive vesicles were concentrated in three different areas within cells: cytoplasmatic pools in the Golgi region (*A*), small pools close to the plasmatic membrane of the cell body (*B*), and large pools stored in the projections of the cells (*C*). *A–D, insets*, the corresponding low magnification pictures. Images show three classes of positive vesicles for either anti-pYE27 alone (*arrowheads*), anti-pYE17 alone (*needles*), or a combination of both antibodies (*arrows*). *E*, quantitative results obtained from sections labeled first with anti-pYE17 (10-nm gold particles) and then with anti-pYE27 (25-nm gold particles). Mean percentages represent the proportion of a particular positive vesicle compared with the total number of positive vesicles observed per micrograph, independently of the location of the pool.

143.7 ± 4.9 nm, respectively. The diameter of double-positive vesicles was greater than the diameter of vesicle containing one peptide ($p < 0.05$).

Initial Cleavage of Pro-TRH Is Key for Differential Sorting of N- and C-terminal Pro-TRH-derived Peptides—Using transfected AtT20 cells, we demonstrated earlier that pro-TRH still undergoes processing when the initial pro-TRH cleavage by PC1/3 is compromised, but the peptides products are not efficiently sorted to SGs (22). Therefore, the question was whether this initial cleavage determines the differential sorting of pro-TRH-derived peptides. First, we determined the N- and C-terminal pro-TRH-derived peptides produced by this mutant. Analysis by RIA of HPLC samples revealed that N- and C-terminal pro-TRH peptides were fully processed in a manner similar to that seen for the wild type pro-TRH (Fig. 5, *A–D*, compare with Fig. 2, *A–D*). Absolute moles of peptide secreted under each treatment are summarized in Table 2, and -fold simulation responses are shown in Fig. 5. The amount of N-terminal peptides in the cell content was higher than for C-terminal peptides (97.0 ± 10.1 *versus* 50.2 ± 5.4 fmol/mg of protein, respectively, $p < 0.05$). Basal secretion for N-terminal peptides was also higher than C-terminal peptides (197.8 ± 19.3 *versus* 67.7 ± 5.9 fmol/ml, respectively, $p < 0.05$). NE failed to induce pro-TRH-derived peptide secretion. Under KCl (56 mM) treatment, secretion of N- and C-terminal peptides was 257.9 ± 45.0 and 91.7 ± 14.8 fmol/ml, respectively. Consequently, the -fold stimulation levels for N- and C-terminal pro-TRH-derived peptides were 1.30 ± 0.23 *versus* 1.35 ± 0.22, respectively (Fig. 5*F*). SI for N- and C-terminal peptides was 0.13 ± 0.05 and 0.02 ± 0.16, respectively, suggesting that they were not efficiently sorted to SGs (Table 2).

Using the same experimental conditions described above, we found that in AtT20 cells expressing PC1/3-block pro-TRH, the number of positive vesicles represented 49.0 ± 7.7% per cell per section. This percentage was similar to the value observed in cells expressing wild type pro-TRH, suggesting that results were not affected by a detection problem. These cells had the same three

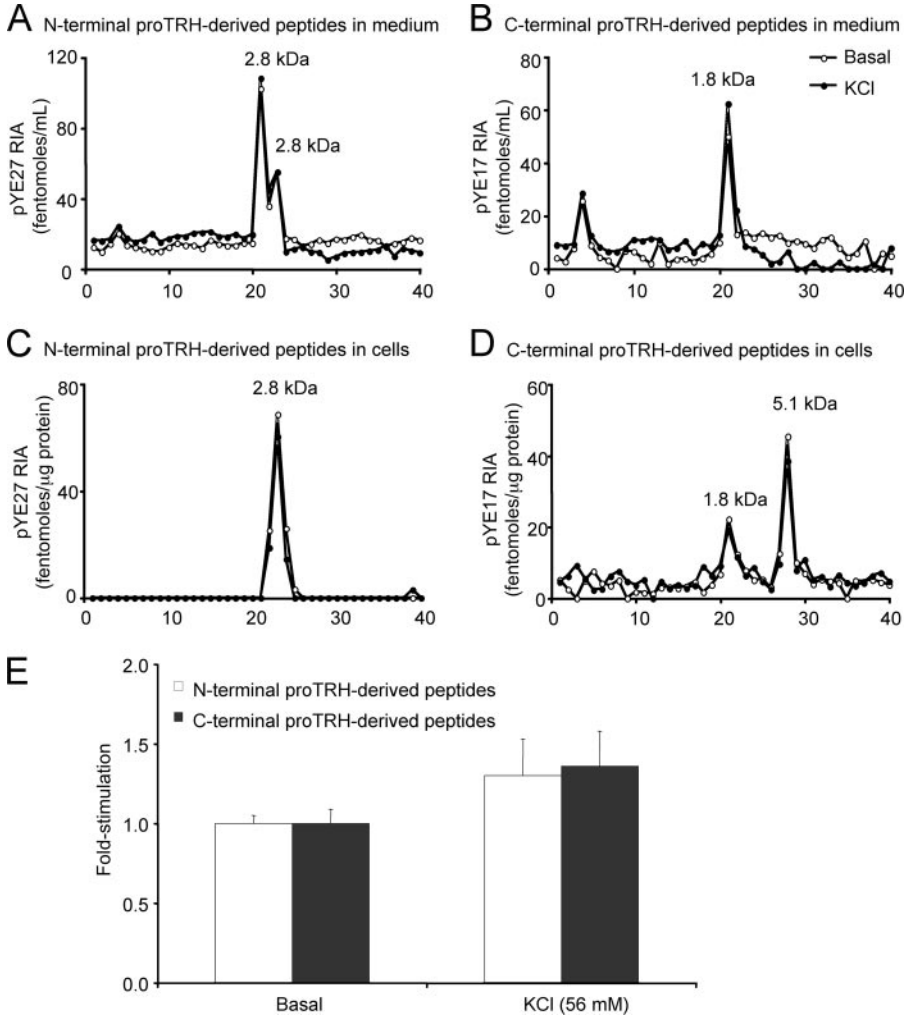

FIGURE 5. **AtT20 cells stably transfected with PC1/3-block prepro-TRH cDNA produce the same N- and C-terminal pro-TRH-derived peptides; however, they are sorted to the constitutive pathway.** Medium and cell content of AtT20 cells expressing PC1/3-Block pro-TRH under basal or KCl (56 mM) treatment were collected and subjected to HPLC purification, and fractions were analyzed using pYE27 and pYE17 RIAs. *A–D*, the *upper panels* show the results of medium samples analyzed with pYE27 (*A*) or pYE17 (*B*) RIAs; the *middle panels* show the results of cell content samples analyzed with pYE27 (*C*) or pYE17 (*D*) RIAs. *E*, -fold stimulation for both peptides calculated as total molar amount of peptide in stimulated media/molar amount of peptide in basal media. Data are presented as mean ± S.E.

TABLE 2

Secretion of N- and C-terminal pro-TRH-derived peptides by AtT20 cells stably transfected with PC1/3-block prepro-TRH cDNA

The first two columns of values show peptides released after 1 h of treatment with the different secretagogues. They are expressed as the total fmol of N- or C-terminal pro-TRH-derived peptides per ml of medium. Both peptides were measured by RIA. SI was calculated as indicated in the text.

Secretagogue	Pro-TRH-derived peptides in medium	
	N-terminal	C-terminal
	fmol/ml	
Basal	197.8 ± 19.3	67.7 ± 5.9[a]
KCl (56 mM)	257.9 ± 45.0	91.7 ± 14.8[a]
SI	0.13 ± 0.05	0.02 ± 0.16

[a] $p < 0.05$ *vs.* total fmol of N-terminal pro-TRH-derived peptides.

classes of immunoreactive vesicles, distributed in the same type pools, as seen in cells expressing wild type pro-TRH (Fig. 6, *A–D*). However, the relative percentages were different. For the mutant, 0.9 ± 0.4 and 15.3 ± 1.9% of total positive vesicles were positive for anti-pYE27 and anti-pYE17 antibodies, respectively ($p < 0.05$ *versus* cells expressing wild type pro-TRH; Fig. 6*E*). In contrast, 81.7 ± 7.4% of total positive vesicles were positive for both antibodies ($p < 0.05$ *versus* cells expressing wild type pro-TRH; Fig. 6*E*). The diameter of positive vesicles for anti-pYE27 alone, for anti-pYE17 alone, and for both antibodies was 111.6 ± 4.4, 117.2 ± 3.0, and 160.2 ± 7.9 nm, respectively. The diameter of double-positive vesicles was greater than the diameter of vesicles containing only one peptide ($p < 0.05$), similar to results seen in cells expressing wild type pro-TRH. These results suggest that differential sorting of pro-TRH-derived peptides is affected when pro-TRH is not efficiently processed at the TGN level.

N- and C-terminal Pro-TRH-derived Peptides Are Differentially Packed and Secreted in Vivo—To establish the relevance of differential sorting *in vivo*, we studied the distribution of N- and C- terminal peptides in the hypothalamic ME, where axon terminals derived from the hypothalamic paraventricular nucleus release pro-TRH-derived peptides to the circulation. The data showed that ME contains and secretes the same peptides found in transfected AtT20 cells (Fig. 7, compare with Fig. 2, *A–D*). Absolute moles of peptide secreted under each treatment are summarized in Table 3, and -fold simulation responses are shown in Fig. 7. Basal secretion for N-terminal peptides was higher than for C-terminal peptides (89.0 ± 3.8 *versus* 39.1 ± 1.0 fmol/ml, respectively, $p < 0.05$), and the ratio between N- and C-terminal peptides was 2.28 ± 0.12. Treatment with NE (500 nM) increased C-terminal peptides release to 54.7 ± 2.2 fmol/ml (1.40- ± 0.06-fold, $p < 0.05$ *versus* basal), but secretion of N-terminal peptides was not affected (86.6 ± 2.4 fmol/ml). Under these experimental conditions hypothalamic explants showed a modest response to NE, which is consistent with an earlier report using a similar system (35). KCl increased N- and C-terminal peptide release rates to 160.9 ± 9.1 and 122.6 ± 10.3 fmol/ml, respectively ($p < 0.05$ *versus* basal). However, KCl-induced stimulation was differential, because it increased more secretion of C-terminal than N-terminal peptides (3.14- ± 0.26-fold *versus* 1.81- ± 0.10-fold, respectively; Fig. 7, Table 3, $p < 0.05$). The SI parameter was higher for C- than for N- terminal pro-TRH-

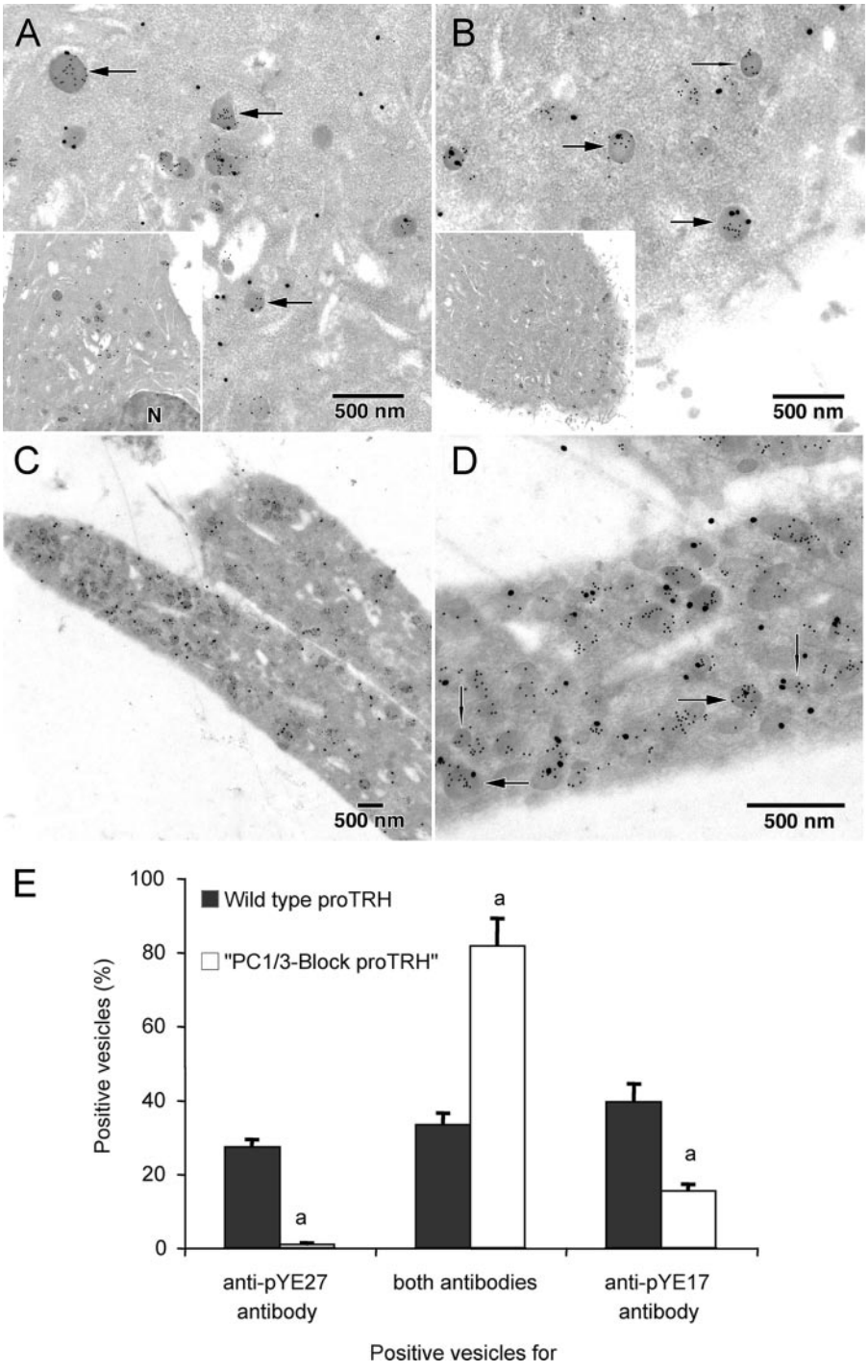

FIGURE 6. **AtT20 cells stably transfected with PC1/3-Block prepro-TRH cDNA sort N- and C-terminal pro-TRH-derived peptides to the same vesicles.** Cells expressing PC1/3-Block pro-TRH were fixed with 4% paraformaldehyde/0.15% glutaraldehyde solution and labeled with anti-pYE17 (visualized with 10-nm gold particle secondary antibody) followed by anti-pYE27 (visualized with 25-nm gold particle secondary antibody). Positive vesicles were concentrated in three different areas within cells: cytoplasmatic pools in the Golgi region (*A*), small pools close to the plasmatic membrane of the cell body (*B*), and large pools stored in the projections of the cells (*C* and *D*, which show low and high magnification, respectively, of the same area). *Insets* in *A* and *B* show the corresponding low magnification views. Images show mostly positive vesicles for a combination of both antibodies (*arrows*). *E*, quantitative results obtained from sections. Mean percentages represent the proportion of a particular positive vesicle compared with the total number of positive vesicles observed per micrograph, independently of the location of the pool. Data are presented as mean ± S.E. *a*, $p < 0.05$ *versus* cells expressing wild type pro-TRH (see Fig. 4).

derived peptides (2.74 ± 0.43 and 1.09 ± 0.14, respectively, $p < 0.05$), suggesting that C-terminal peptides were also more efficiently sorted to the RSP *in vivo*.

We then determined the distribution of N- and C-terminal pro-TRH-derived peptides within the ME using an IEM approach. Under Karnovsky's fixative the ultrastructure of tissue was well preserved. In the external layer of the ME, we observed different classes of vesicles: small, small dense core, and large dense core vesicles. However, antibodies failed to label them (Fig. 8*A*). Therefore, we used a 4% paraformaldehyde/0.15% glutaraldehyde solution, which maintained antigenicity, although the ultrastructure was not as well preserved. Under these conditions, staining was seen in large dense core vesicles typically arranged in clusters within the axons (Fig. 8, *B–D*). In the ME, 15.3 ± 4.2% of the vesicle clusters exhibited antibody binding, and both species of colloidal gold-tagged antibodies were found in all of the stained clusters. In the ME, the diameter of positive dense core vesicles for anti-pYE27, for anti-pYE17, and for both antibodies was 69.1 ± 3.2, 73.0 ± 3.6, and 72.7 ± 2.7 nm, respectively. Quantitative analysis showed three classes of immunoreactive vesicles (Fig. 8*E*). One class was positive for anti-pYE27 and represented 33.4 ± 3.3% of the total positive vesicles. Another class was positive for anti-pYE17 and represented 44.3 ± 3.1% of the total positive vesicles. A third population of vesicles was positive for both antibodies and represented 22.2 ± 2.3% of the total positive vesicles.

DISCUSSION

This is the first study showing that a mammalian prohormone such as pro-TRH, initially cleaved in the TGN by PC1/3, can deliver its products to different vesicles of the secretory pathway. This is supported by the fact that N- and C-terminal pro-TRH-derived peptides are differentially secreted under specific and unspecific secretagogue stimulation and by the evidence of distinct distribution of peptides within the secretory vesicles. Furthermore, obliteration of the initial cleavage by PC1/3 on pro-TRH was shown to be critical in the targeting of N- and C-

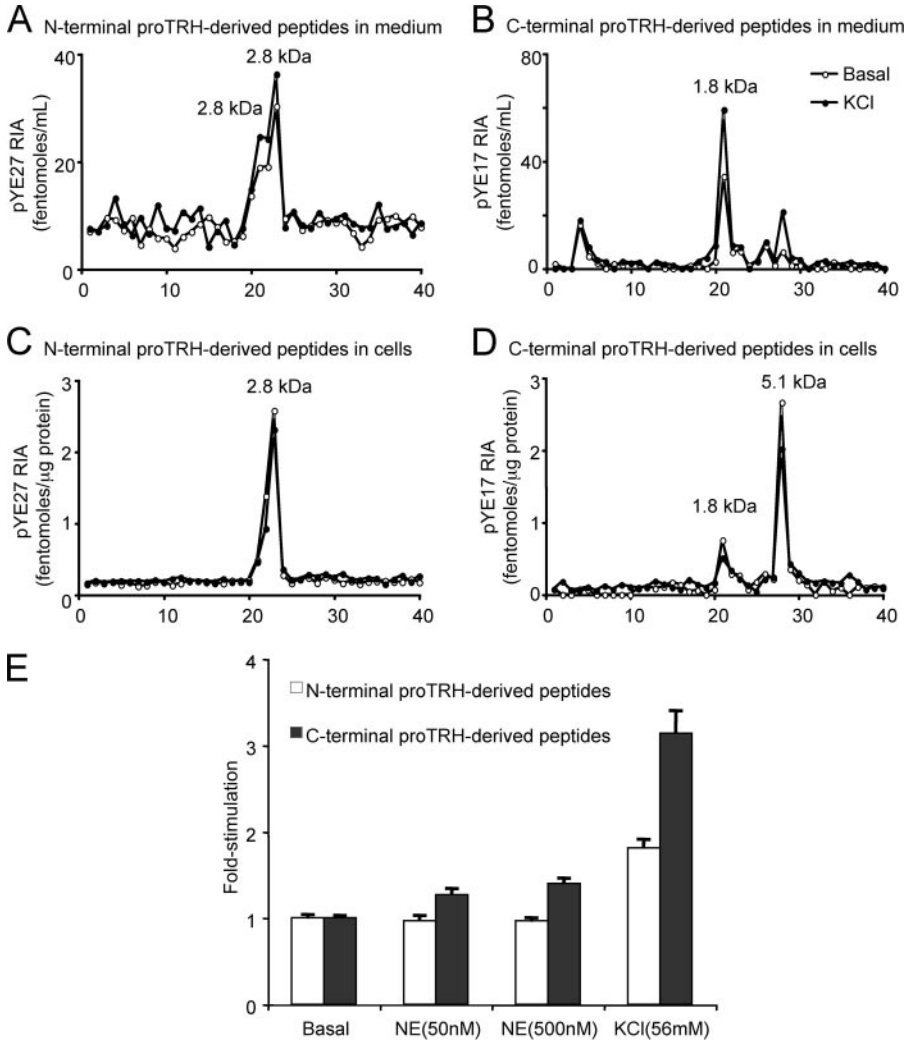

FIGURE 7. **NE and KCl induce a differential release of N- *versus* C-terminal pro-TRH-derived peptides in hypothalamic explants.** Cell content and release of hypothalamic explants under basal, NE (50–500 nM), or KCl (56 mM) treatment were collected and subjected to HPLC purification, and fractions were analyzed using pYE27 and pYE17 RIAs. The *upper panels* show the results of basal and KCl-stimulated medium samples analyzed with pYE27 (*A*) or pYE17 (*B*) RIAs; the *middle panels* show the results of basal and KCl-stimulated cell content samples analyzed with pYE27 (*C*) or pYE17 (*D*) RIAs. *E*, -fold stimulation for both peptides calculated as total molar amount of peptide in stimulated media/molar amount of peptide in basal media. Data are presented as mean ± S.E. *a*, $p < 0.05$ *versus* own basal release. *b*, $p < 0.05$ *versus* -fold stimulation of N-terminal pro-TRH-derived peptide for the same stimulus.

TABLE 3

Secretion of N- and C-terminal pro-TRH-derived peptides by hypothalamic explants

The first two columns of values show peptides released after 1 h of treatment with the different secretagogues. They are expressed as the total fmol of N- or C-terminal pro-TRH-derived peptides per ml of medium. Both peptides were measured by RIA. SI was calculated as indicated in the text.

Secretagogue	Pro-TRH-derived peptides in medium	
	N-terminal	C-terminal
	fmol/ml	
Basal	89.0 ± 3.8	39.1 ± 1.0[a]
NE (50 nM)	86.3 ± 4.9	48.2 ± 2.4[a,b]
NE (500 nM)	86.6 ± 2.4	54.7 ± 2.2[a,b]
KCl (56 mM)	160.9 ± 9.1[b]	122.6 ± 10.3[a,b]
SI	1.09 ± 0.14	2.74 ± 0.43[c]

[a] $p < 0.05$ *vs.* total fmol of N-terminal pro-TRH-derived peptides.
[b] $p < 0.05$ *vs.* basal.
[c] $p < 0.05$ *vs.* SI of N-terminal pro-TRH-derived peptides.

terminal peptides to different vesicles. This could represent an essential mechanism for independent regulation of the secretion of different bioactive peptides derived from the same prohormone.

Synthesis of prohormone polypeptides and their processing to end products occur while they are sorted to the SGs (1–4). The correct sorting events of proteins and peptides to their target organelles are of fundamental importance in cell biology. However, identification of the signals or physical properties that ensure proper intracellular sorting of peptides to dense core SGs is not yet fully established. In a recent review article, Dikeakos and Reudelhuber (36) subdivided the targeting function of proteins that are sorted to SGs into three groups: membrane-associated (or traversing) tethers, tether-associated cargo, and aggregation. The enzyme PC1/3 is a granule-tethered protein that may act as a sorting chaperone for its substrates in addition to being a processing enzyme. In the case of pro-TRH, we recently showed that initial processing action of PC1/3 on pro-TRH, and not a cargo-receptor relationship, is important for the sorting of the pro-TRH-derived peptides (22). Thus, it is possible that key paired basic amino acids of pro-TRH (residues 107, 108, 113, 114, 152, 153, and 159), which constitute a cleavage site for PC1/3, would also function as granule sorting domains (22, 36).

Our results show that some N- and C-terminal pro-TRH-derived fragments behave independently after the prohormone is cleaved. It is possible that the initial cleavage changes the folding conformation and/or exposes different motifs that allow N- and C-terminal pro-TRH- fragments to aggregate independently or to interact with different components of the RSP. Interestingly, the differential sorting is independent of the cell type. This suggests that the N- and C-terminal ends of pro-TRH have conserved properties, which are sufficient for the sorting events. This also suggests that the cellular environment is not a critical factor, although the presence of RSP machinery should be necessary. Peptides derived from the same precursor, which are differentially packaged, have been shown for the egg-laying hormone (ELH) precursor in both *Aplysia californica* and *Lymnaea stagnalis* (37–39), but this phenomenon had never been demonstrated in mammalian prohormones.

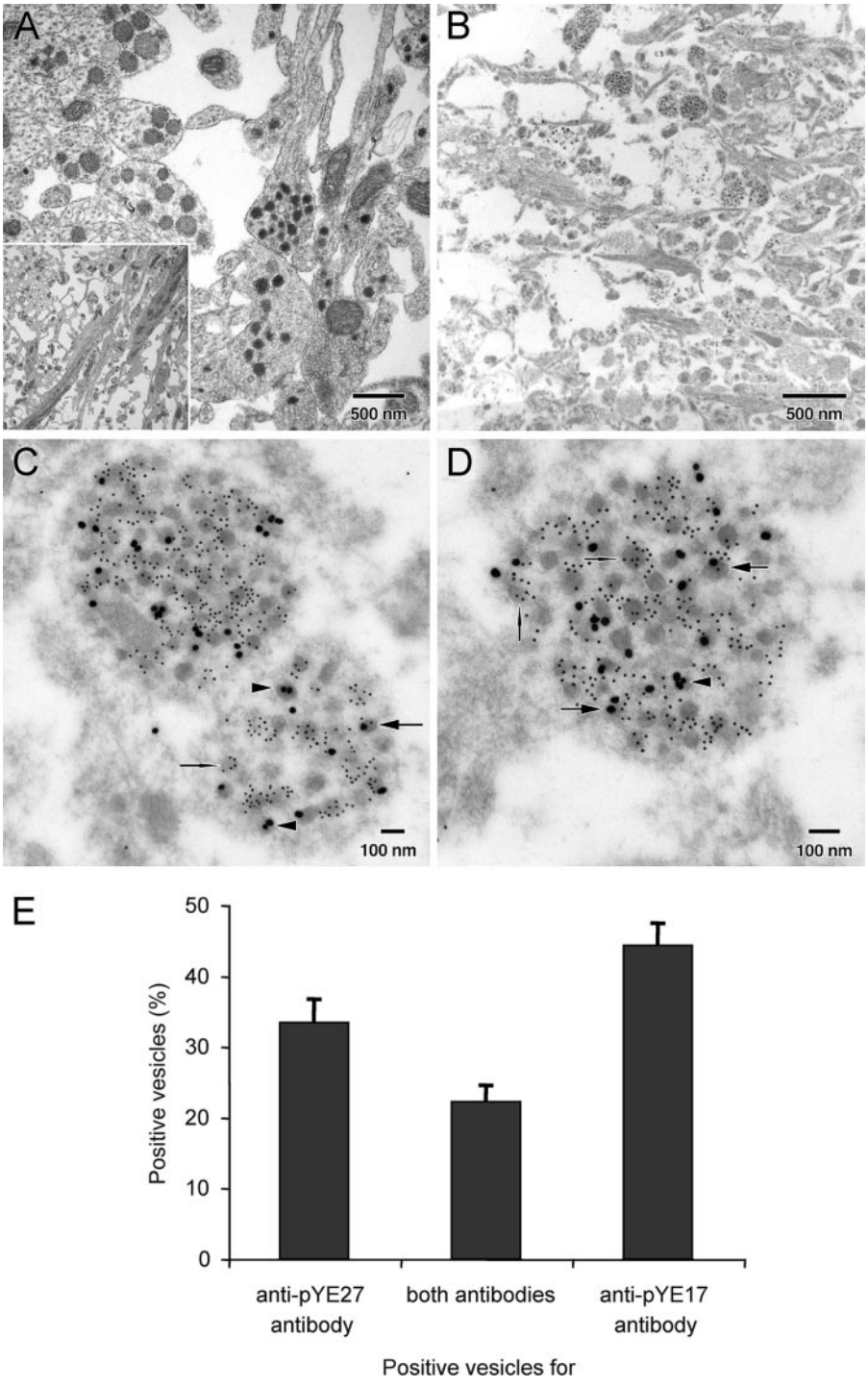

FIGURE 8. **N- and C-terminal end products of pro-TRH are partially located in different vesicles within the ME fibers.** Sprague-Dawley rats were perfused with Karnovsky's fixative (*A, inset*, shows a panoramic micrograph of this region) or with 4% paraformaldehyde/0.15% glutaraldehyde in PBS (*B–D*). *C* and *D* show an increased magnification of *B*. Images show three classes of positive vesicles for anti-pYE17 antibody alone (*arrowheads*), anti-pYE17 antibody alone (*needles*), or a combination of both antibodies (*arrows*). *E*, quantitative results obtained from sections labeled first with anti-pYE17 (10-nm gold particles) and then with anti-pYE27 (25-nm gold particles). Mean percentages represent the proportion of a particular positive vesicle compared with the total number of positive vesicles observed per micrograph.

Pro-TRH producing cells contain a significant number of vesicles that store both N- and C-terminal pro-TRH-derived peptides. However, most of the pro-TRH molecules are initially cleaved in the TGN (21). Thus, it is possible that double-positive vesicles are heterogeneous in their quantitative content, enriched with one peptide but also containing small amounts of other pro-TRH-derived peptides. This possibility fits better with our quantitative release data, which show that N-terminal peptides are highly secreted under basal condition but also are secreted upon stimulation. It has been already shown that SG populations are heterogeneous in their quantitative content of proteins derived from different genes (40), but whether this can also occur with two peptides derived from the same precursor requires further demonstration. Double IEM has been used to quantify the relative content in double-positive vesicles (41, 42); however, there are serious objections to this usage because of steric hindrance problems and differences in labeling efficiency between gold probes of different sizes (33). Interestingly, double-positive vesicles in transfected cells were larger than vesicles containing one peptide. This observation may suggest that double-positive vesicles belong to the group of immature vesicles, but this hypothesis needs to be confirmed. The finding that the molar ratio of N- to C-terminal pro-TRH-derived peptides under steady state conditions was higher than 1 was unexpected based on the biosynthetic pathway of Fig. 1. These peptides are not significantly degraded, either intra- nor extracellularly, as suggested by the fact that bafilomycin A1, an inhibitor of the lysosomal degradation, did not improve the molar ratio and that these synthetic peptides added to the medium were stable in the presence of cells (not shown). Thus, we speculate that this molar ratio is a consequence of the fact that N-terminal intermediate forms are more rapidly processed than C-terminal ones, as we demonstrated using pulse-chase strategies (21). Still, this intriguing observation, which requires further investigation, does not invalidate the differences in -fold stimulation that support the differential secretion.

Secretory cells release peptide content in the SGs upon stimulation. Potassium is an unspecific secretagogue that induces peptide release based on its ability to depolarize cells and

increase cytosolic Ca^{2+} (28). NE is a physiological secretagogue that acts via specific receptors using protein kinase A and Ca^{2+}-dependent intracellular pathways in both neurons and AtT20 cells (35, 43). The secretion of N-terminal peptides was only slightly increased by NE and KCl, suggesting that this peptide is not efficiently stored in secretory vesicles (Figs. 2 and Fig. 7). In contrast, both secretagogues strongly secreted the C-terminal pro-TRH-derived peptides, indicating that these peptides are preferentially stored into SGs. The high SI for the C-terminal peptide quantitatively supports this conclusion (Tables 1 and 3). Recently, we showed that initial processing of pro-TRH by PC1/3 in the TGN is necessary for the correct trafficking of pro-TRH-derived peptides to secretory vesicles (22), and we now show that initial cleavage of pro-TRH in the TGN is also critical for the sorting of N- and C-terminal peptides to different vesicles. Interestingly, PC1/3-block pro-TRH produces the same final N- and C-terminal pro-TRH-derived peptides, but they are constitutively released (SI close to zero), probably because the mutated prohormone is cleaved in a post-TGN compartment (22). Thus, our results suggest that the differential secretion of pro-TRH-related peptides is due to the early processing in the TGN that governs its differential storage, most likely because C-terminal pro-TRH-derived peptides behave independently and can be more efficiently sorted to the RSP than the N-terminal ones.

The pro-TRH sequence contains five copies of the TRH progenitor and another seven pro-TRH-derived peptides, which can be further processed (17, 18). For instance, prepro-TRH-(178–199) peptide is cleaved to give prepro-TRH-(178–184) and prepro-TRH-(186–199) peptides. In this study, we found that ME stores the C-terminal prepro-TRH-(208–255) peptide; however, the main product released is a shorter peptide, prepro-TRH-(241–255). This peptide is likely derived from the cleavage of prepro-TRH-(208–255) at the C-terminal side of the lysine residue at prepro-TRH-(240), which follows the rules that govern monobasic cleavage sites (44). Importantly, we have recently shown that this N-terminal peptide is produced abundantly in the lateral hypothalamus (45). However, its physiological relevance remains unknown. The N-terminal pro-TRH-derived peptide is also intriguing because it is stored as one variant of the N-terminal prepro-TRH-(25–50) (2759 Da) but is released as two different variant (2755 and 2759 Da). We have evidence that the N-terminal segment, prepro-TRH-(25–50), plays a conformational role in the initial folding of the pro-TRH[3]; this possibility is consistent with its constitutive release. However, the significance of these late and undetermined post-transcriptional modifications remains unknown. For other prohormones the same mechanism of differential sorting may occur. For instance, proghrelin generates two peptide hormones with antagonist actions: ghrelin increases food intake and body weight, whereas obestatin has the opposite action (46, 47). Similarly, pro-opiomelanocortin (POMC) produces two POMC-derived peptides, α-melanocyte-stimulating hormone and opioids, which have opposite actions on body weight and appetite (48–50). In conclusion, here we have demonstrated that peptides derived from the N- and C-terminal sides of pro-TRH can be differentially sorted and secreted. This is a novel aspect of the biology of pro-TRH that also may have important implications for the study of other prohormones.

[3] A. Romero, I. Cakir, C. A. Vaslet, R. C. Stuart, O. Lansari, H. A. Lucero, and E. A. Nillni, manuscript submitted for publication.

Acknowledgments—We thank Carol Ayala and Virginia Hovanesian for assistance in the generation of IEM and presentation of the images.

REFERENCES

1. Arvan, P., and Castle, D. (1998) *Biochem. J.* **332,** 593–610
2. Seidah, N. G., and Chretien, M. (1997) *Curr. Opin. Biotechnol.* **8,** 602–607
3. Steiner, D. F. (1998) *Curr. Opin. Chem. Biol.* **2,** 31–39
4. Glombik, M. M., and Gerdes, H. H. (2000) *Biochimie* (*Paris*) **82,** 315–326
5. Traub, L. M., and Kornfeld, S. (1997) *Curr. Opin. Cell Biol.* **9,** 527–533
6. Borgonovo, B., Ouwendijk, J., and Solimena, M. (2006) *Curr. Opin. Cell Biol.* **18,** 365–370
7. Nillni, E. A., Sevarino, K. A., and Jackson, I. M. (1993) *Endocrinology* **132,** 1271–1277
8. Xu, H., and Shields, D. (1994) *Biochimie* (*Paris*) **76,** 257–264
9. Villeneuve, P., Seidah, N. G., and Beaudet, A. (2000) *Neuroreport* **11,** 3443–3447
10. Perone, M. J., Murray, C. A., Brown, O. A., Gibson, S., White, A., Linton, E. A., Perkins, A. V., Lowenstein, P. R., and Castro, M. G. (1998) *Mol. Cell. Endocrinol.* **142,** 191–202
11. Schnabel, E., Mains, R. E., and Farquhar, M. G. (1989) *Mol. Endocrinol.* **3,** 1223–1235
12. Wattenberg, B. W. (1990) *J. Cell. Physiol.* **143,** 287–293
13. Tooze, J., Hollinshead, M., Frank, R., and Burke, B. (1987) *J. Cell. Biol.* **105,** 155–162
14. Tanaka, S., Nomizu, M., and Kurosumi, K. (1991) *J. Histochem. Cytochem.* **39,** 809–821
15. Schmidt, W. K., and Moore, H. P. (1995) *Mol. Biol. Cell* **6,** 1271–1285
16. Nillni, E. A., Sevarino, K. A., and Jackson, I. M. (1993) *Endocrinology* **132,** 1260–1270
17. Nillni, E. A., and Sevarino, K. A. (1999) *Endocr. Rev.* **20,** 599–648
18. Perello, M., and Nillni, E. (2007) *Front. Biosci.* **12,** 3554–3565
19. Nillni, E. A., Friedman, T. C., Todd, R. B., Birch, N. P., Loh, Y. P., and Jackson, I. M. (1995) *J. Neurochem.* **65,** 2462–2472
20. Schaner, P., Todd, R. B., Seidah, N. G., and Nillni, E. A. (1997) *J. Biol. Chem.* **272,** 19958–19968
21. Perez de la Cruz, I., and Nillni, E. A. (1996) *J. Biol. Chem.* **271,** 22736–22745
22. Mulcahy, L. R., Vaslet, C. A., and Nillni, E. A. (2005) *J. Biol. Chem.* **280,** 39818–39826
23. Nillni, E. A., Aird, F., Seidah, N. G., Todd, R. B., and Koenig, J. I. (2001) *Endocrinology* **142,** 896–906
24. Goldstein, J., Perello, M., and Nillni, E. A. (2007) *J. Mol. Neurosci.* **31,** 69–82
25. Nillni, E. A., Lee, A., Legradi, G., and Lechan, R. M. (2002) *J. Neurochem.* **80,** 874–884
26. Bulant, M., Roussel, J.-P., Astier, H., Nicolas, P., and Vaudry, H. (1990) *Proc. Natl. Acad. Sci. U. S. A.* **87,** 4439–4443
27. Aoki, Y., Iwasaki, Y., Katahira, M., Oiso, Y., and Saito, H. (1997) *Endocrinology* **138,** 1923–1929
28. Mains, R. E., and Eipper, B. A. (1981) *J. Cell Biol.* **89,** 21–28
29. Reisine, T. D., Heisler, S., Hook, V. Y., and Axelrod, J. (1983) *J. Neurosci.* **3,** 725–732
30. Schmidt, W. K., and Moore, H.-P. (1994) *J. Biol. Chem.* **269,** 27115–27124
31. Perello, M., Stuart, R. C., and Nillni, E. A. (2006) *Endocrinology* **147,** 3296–3306
32. Josic, D., Brown, M. K., Huang, F., Callanan, H., Rucevic, M., Nicoletti, A., Clifton, J., and Hixson, D. C. (2005) *Electrophoresis* **26,** 2809–2822
33. Merighi, A. (1992) in *Electron Microscopic Immunocytochemistry: Principles and Practice* (Polak, J. M., and Priestley, J. V., eds) pp. 51–87, Oxford University Press, New York
34. Tooze, J., Tooze, S. A., and Fuller, S. D. (1987) *J. Cell Biol.* **105,** 1215–1226

35. Tapia-Arancibia, L., Arancibia, S., and Astier, H. (1985) *Endocrinology* **116,** 2314
36. Dikeakos, J. D., and Reudelhuber, T. L. (2007) *J. Cell Biol.* **177,** 191–196
37. Fisher, J. M., and Scheller, R. H. (1988) *J. Biol. Chem.* **263,** 16515–16518
38. Sossin, W. S., Fisher, J. M., and Scheller, R. H. (1990) *J. Cell Biol.* **110,** 1–12
39. van Heumen, W. R., and Roubos, E. W. (1991) *Cell Tissue Res.* **264,** 185–195
40. Sobota, J. A., Ferraro, F., Back, N., Eipper, B. A., and Mains, R. E. (2006) *Mol. Biol. Cell* **17,** 5038–5052
41. Klumperman, J., Spijker, S., van Minnen, J., Sharp-Baker, H., Smit, A. B., and Geraerts, W. P. (1996) *J. Neurosci.* **16,** 7930–7940
42. Fisher, J. M., Sossin, W. S., Neucomb, R., and Scheller, R. H. (1988) *Cell* **54,** 813–822
43. Cote-Velez, A., Perez-Martinez, L., Diaz-Gallardo, M. Y., Perez-Monter, C., Carreon-Rodriguez, A., Charli, J. L., and Joseph-Bravo, P. (2005) *J. Mol. Endocrinol.* **34,** 177–197
44. Devi, L. (1991) *FEBS Lett.* **280,** 189–194
45. Perello, M., Friedman, T., Paez-Espinosa, V., Shen, X., Stuart, R. C., and Nillni, E. A. (2006) *Endocrinology* **147,** 2705–2716
46. Tschop, M., Smiley, D. L., and Heiman, M. L. (2000) *Nature* **407,** 908–913
47. Zhang, J. V., Ren, P. G., Avsian-Kretchmer, O., Luo, C. W., Rauch, R., Klein, C., and Hsueh, A. J. (2005) *Science* **310,** 996–999
48. Cone, R. D. (2005) *Nat. Neurosci.* **8,** 571–578
49. Glass, M. J., Billington, C. J., and Levine, A. S. (1999) *Neuropeptides* **33,** 360–368
50. Diano, S., Kalra, S. P., and Horvath, T. L. (1998) *J. Neuroendocrinol.* **10,** 647–650